Evidence of Nonlocal Breakdown of the Integer Quantum Hall Effect

S. Komiyama and Y. Kawaguchi
Department of Pure and Applied Science, University of Tokyo, Komaba 3-8-1, Meguro-ku, Tokyo, Japan

T. Osada and Y. Shiraki
Research Center of Advanced Science and Technology, University of Tokyo, Komaba 3-6-1, Meguro-ku, Tokyo, Japan
(Received 25 March 1996)

Current induced breakdown of the integer quantum Hall effect (QHE) is studied in GaAs/AlGaAs single heterostructure Hall bars at $T = 1.6–4.2$ K and $B = 2–6$ T ($\nu = 2$, 4, and 6). The QHE breakdown is absent over a macroscopic region in the two-dimensional electron gas channel on the side of the electron-injecting corner of the Hall bars. The observed nonlocal nature suggests that bootstrap-type electron heating is relevant to the QHE breakdown. [S0031-9007(96)00600-X]

PACS numbers: 73.40.Hm, 72.20.Ht, 72.20.My

Integer quantum Hall effects (QHE) are remarkable phenomena of two-dimensional electron gas (2DEG) systems, in which the longitudinal resistance R_x vanishes while the Hall resistance R_H is quantized to integer multiples of h/e^2 [1,2]. The longitudinal resistance R_x abruptly increases to destroy the dissipationless QHE states when the current passing through a device exceeds a critical value [3,4]. Although a variety of characteristics of the QHE breakdown have been revealed by a number of experiments [5–15], the mechanism of the breakdown has not yet been fully understood.

At present, two different categories of the QHE breakdown are experimentally distinguished for 2DEG systems in GaAs/AlGaAs heterostructures. In one category, the critical current I_c scales linearly with the device width W, readily exceeding 10 μA when $W > 20$ μm [13]. In the other category I_c scales sublinearly with W, not exceeding 10 μA even for wider devices of $W > 100$ μm [11]. The distinction does not appear to rigidly relate to the 2DEG mobility [16], but may possibly reflect wafer-specific electron-density fluctuations [15]. In this Letter, we focus our attention mainly on the first category of the QHE breakdown, and report novel characteristics using Hall-bar devices with voltage probes placed asymmetrically with respect to the current contacts. We find that, even when a current exceeding I_c is passed through a Hall-bar device, the longitudinal voltage V_x along the 2DEG channel is small, or remains practically vanishing, in a region close to an electron-injecting corner of the device, but grows to exhibit well-defined breakdown characteristics as the distance from the electron-injecting corner increases. The relevant characteristic length reaches as large value as 100 μm in high-mobility samples. The experimental data indicate that this macroscopic nonlocality is an intrinsic nature of the QHE breakdown at least of the first category, and strongly restricts possible relevant mechanisms of the QHE breakdown. We will suggest that the nonlocal nature reported here supports an earlier proposed model of the bootstrap-type electron heating (BSEH) [5,6].

Samples were fabricated from two wafers of modulation doped $Al_{0.3}Ga_{0.7}As/GaAs$ single heterostructures, which have proved in the previous work to give rise to the first category of breakdown [16,17], in which I_c linearly scales with W. The 4.2k mobility of 2DEG, μ_H, and the 2DEG sheet density n_s are $\mu_H = 80$ m^2/V s and $n_s = 2.6 \times 10^{15}$/m^2 in one wafer (here-after designated as wafer 1) and $\mu_H = 10$ m^2/V s and $n_s = 5.2 \times 10^{15}$/m^2 in the other wafer (designated as wafer 2). Samples were defined photolithographically and patterned into Hall bars through wet etching as shown in Figs. 1(a) and 1(b). The 2DEG channel is widened to form 2DEG pad regions at the opposite ends, to which Ohmic current contacts are attached. Several pairs of voltage probes are placed nonequidistantly along the 2DEG channel. The lithographical width of each voltage-probe arm is 2 μm

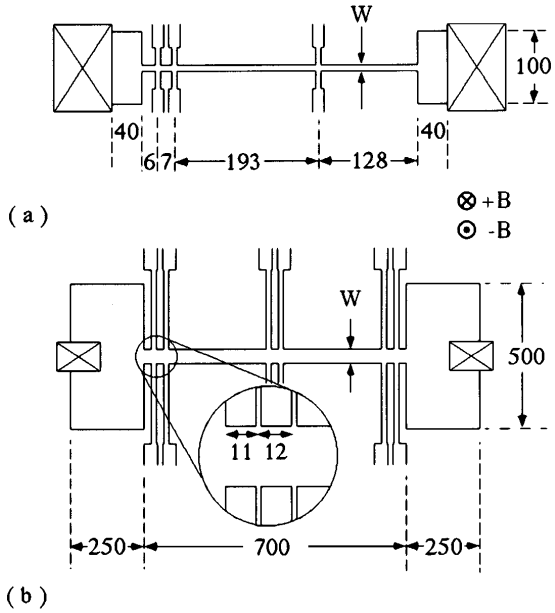

FIG. 1. Hall bars used. The dimensions are given by numbers in units of μm.

 0031-9007/96/77(3)/558(4)$10.00

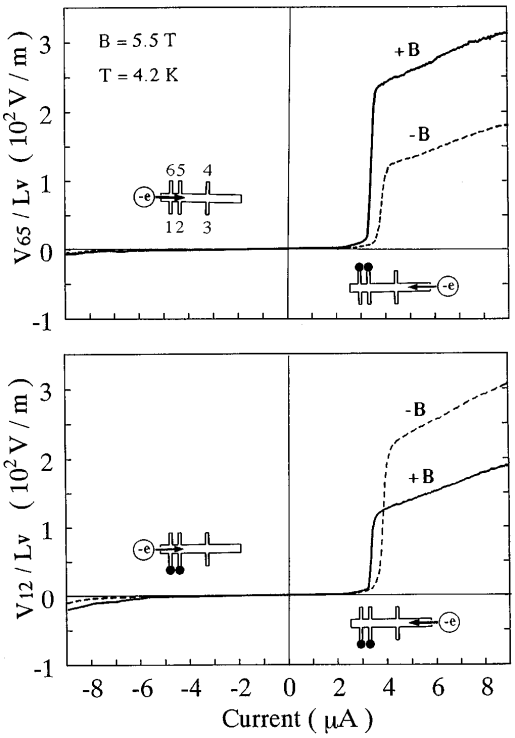

FIG. 2. Longitudinal voltages V_{65} and V_{12} vs I. The polarities of magnetic field ($\pm B$) are indicated in Fig. 1.

in all the devices. Ohmic contacts are prepared by alloying with Au/Ge at 430 °C.

The data in Fig. 2 are taken from a sample patterned from wafer 1 into the shape and the dimensions given in Fig. 1(a) with a lithographic channel width of $W = 3.0\ \mu$m. The voltage probes are numbered in the left-side inset of the upper panel. The upper panel shows the longitudinal voltage V_{65} between the voltage probes 6 and 5 at $T = 4.2$ K by the values normalized by the interprobe distance $L_V = 7\ \mu$m as a function of current I passing through the 2DEG channel for the opposite current polarities. The magnetic field $B = 5.5$ T corresponds to the center of the Landau level filling factor of $\nu = 2$. The voltage V_{65} sharply increases at a critical current of about $I_c = 3\ \mu$A to exhibit well-defined breakdown characteristics when the current polarity is such that electrons are injected from the contact at the right end as indicated by the right-side inset of Fig. 2(a). However, the increase in V_{65} is dramatically suppressed, and any discernible sign of the breakdown disappears for the opposite polarity of current in which electrons are injected from the closer contact at the left end. Throughout this paper, we define the current I as positive when electrons are injected from the contact at the right end and as negative when injected from the contact at the left end. This marked asymmetry is substantially independent of the polarity of magnetic field as shown by the solid and the dotted lines [18]. [The polarities meant by $\pm B$ are indicated in Fig. 1(a).] The lower panel of Fig. 2 indicates that this marked asymmetry is kept unchanged when the voltage probes are interchanged with probes 1 and 2, placed on the opposite side of the 2DEG channel.

The fact that the marked asymmetry is substantially independent of the magnetic field polarity and the side of the 2DEG channel on which the voltage is studied indicate that (i) edge states are irrelevant and (ii) inhomogeneities of the 2DEG in the device are also irrelevant to the observed current-polarity dependence.

The remarkable current-polarity dependence is noted as well in the Hall resistance. The top panels of Figs. 3(a) and 3(b) compare the Hall resistances $R_H = V_{61}/I$ studied at 4.2 K in the opposite polarities of I in the sweep of magnetic field. The magnetic fields are positive ($+B$). The bottom panels compare the longitudinal voltages $|V_{65}|$. The quantized Hall-resistance plateaus and the regions of zero-longitudinal voltages in the Shubnikov–de Hass (SdH) oscillations completely vanish when I exceeds 3 μA in the positive polarity as shown in Figs. 3(a). However, Figs. 3(b) demonstrate that the quantized Hall-resistance plateaus as well as the distinct minima in the SdH oscillations are retained even when $|I|$ exceeds 3 μA in the negative polarity. Additional experiments confirmed that these features are, again, unaffected by the reversal of magnetic fields.

We have simultaneously studied longitudinal voltages in a longer 2DEG channel region further away from the junction corner by using probe pairs of (5,4) and (2,3). The top and bottom panels of Fig. 4 show, respectively, the voltages V_{54} and V_{23} with the values normalized by the interprobe distance $L_V = 193\ \mu$m against $\pm I$. The voltages V_{54} and V_{23} start increasing with increasing I beyond about 3 μA for both polarities of current. However, the increase is distinctly smoother for the negative polarity of I. This current polarity dependence

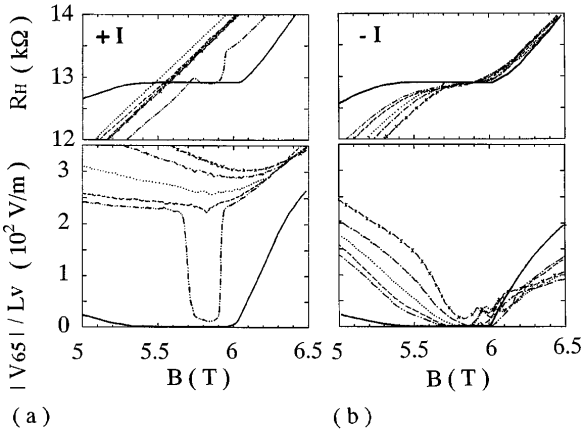

FIG. 3. Hall resistance $R_H = V_{61}/I$ (upper panels) and longitudinal voltages V_{65} (lower panels), against magnetic field, for (a) the positive and (b) the negative polarities of current. $T = 4.2$ K, and the magnetic fields are positive ($+B$). $I = 1(-)$, $3(- \cdot\cdot -)$, $3.5(- - -)$, $5(\cdot\cdot\cdot)$, $7(- \cdot -)$, and $9\ \mu$A$(- \times -)$.

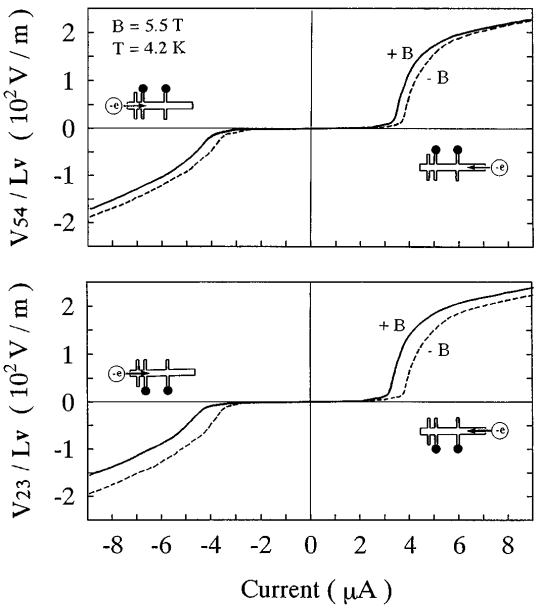

FIG. 4. Longitudinal voltages V_{54} (upper panel) and V_{23} (lower panel) vs $\pm I$.

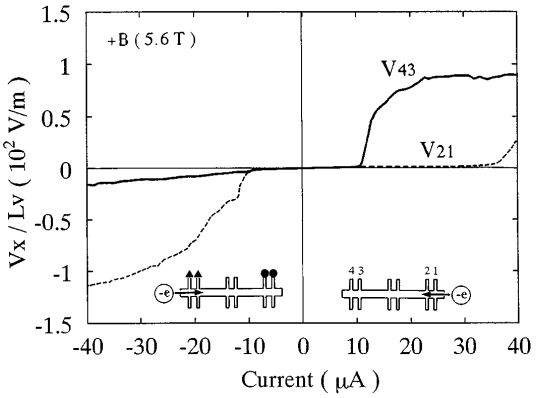

FIG. 5. Longitudinal voltages V_{43} and V_{21} in the 20 μm wide Hall bar, as a function of $\pm I$.

is, again, substantially independent of the reversal of magnetic field or the interchange of the voltage probes. Furthermore, even for the positive polarity of I, the feature of the transition from the QHE regime to the breakdown regime represented by the curves of V_{54} or V_{23} versus I is smoother, when compared to the step-wise transition exhibited by V_{65} or V_{12} in Fig. 2. These observations strongly suggest that a surprisingly large distance L_B, in excess of 130 μm, is necessary, when measured from the electron injecting corner, for the QHE breakdown to fully develop in the 2DEG channel.

The data described above are taken from a relatively narrow Hall bar. To examine whether the observed characteristics are device-width specific, we have fabricated from wafer 1 wider samples with $W = 20$ μm, which have the shape and the dimensions shown in Fig. 1(b). Figure 5 displays longitudinal voltages V_{43} and V_{21} with the values normalized by the interprobe distance $L_V = 12$ μm as a function of $\pm I$ for the magnetic field B corresponding to $\nu = 2$. The voltage probes, 1–4, used for the measurements are marked in the insets of the figure. For the positive polarity of I, the voltage V_{43} exhibits well-defined breakdown characteristics while they are not clearly discerned in the other voltage V_{21} [19]. These features are reversed for the negative polarity of I. We have confirmed in additional experiments that these characteristics are again independent of the polarity of B and the side of the 2DEG channel on which the voltage probes are attached.

In all the devices, similar characteristics were also observed at lower magnetic fields corresponding to the filling factors of $\nu = 4$ and 6, where the characteristic lengths L_B of the QHE breakdown were found to reduce to the order of $L_B \sim 20$ μm for $\nu = 4$ and less than 10 μm for $\nu = 6$. We have also studied temperature dependence and found that the current-polarity dependent characteristics of the QHE breakdown, including the size of the characteristic lengths L_B, do not strongly depend on the T in the range between 4.2 and 1.6 K.

To study sample dependence, we have fabricated 2.4 μm wide Hall bars with the shape and the dimensions shown in Fig. 1(b) from wafer 2. These lower-mobility devices also showed similar and systematic current-polarity dependence as described above. The size of L_B, however, was found to be distinctly smaller, such that $L_B \sim 10$ μm at $B = 5.4$ T ($\nu = 4$).

The present observations are completely consistent with our previous reports on the device-length dependence of the QHE breakdown [16,17] and may explain the earlier report by Bliek *et al.* that the QHE breakdown does not occur in a short constricted 2DEG channel at an expected current level [8]. Moreover, the present experiments further reveal that the QHE breakdown is not occuring in a 2DEG channel region near the electron injecting corner of the device but develops as the injected electrons travel over a macroscopic distance. It is highly probable that this remarkable current-polarity dependent nonlocal nature is intrinsic to the QHE breakdown, at least of the first category.

The total Hall voltage V_H, or the averaged Hall electric field $|E_H| \equiv |V_H|/W = (h/\nu e^2)|I|/W$, in the 2DEG channel is independent of the current polarity. The present experiments, therefore, directly indicate that, in the QHE breakdown, longitudinal conductivity $\sigma_{xx}(r)$ abruptly increases not by being locally affected by the Hall electric filed $E_H(r)$. Thus is may not be easy to explain the breakdown by assuming microscopic mechanisms, e.g., the Zener-type tunneling of electrons to higher Landau levels [20–22], through which $E_H(r)$ directly affects $\sigma_{xx}(r)$.

On this basis, we suggest that the BSEH [5,6,23] is a probable mechanism. The model assumes that $E_H(r)$ in the experimental condition is so small as to cause no appreciable influence on $\sigma_{xx}(r)$ even in a range of

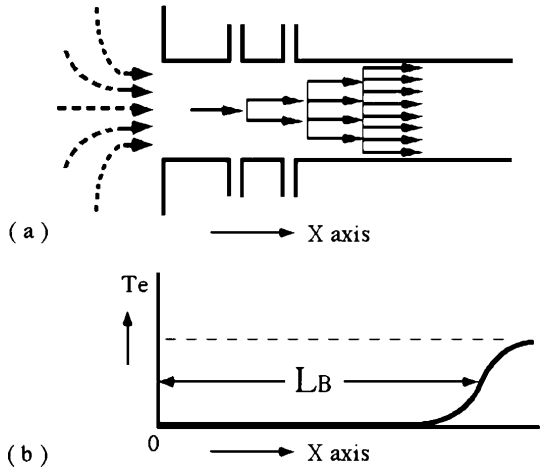

FIG. 6. (a) Cold electron injection into a 2DEG channel (arrows with dotted lines), and avalanche-type multiplication of excited electrons and holes (arrows with solid lines). (b) An exponential increase of T_e, followed by a saturation.

I_c. Instead, the model takes into account the fact that $\sigma_{xx}(r)$ should sensitively depend on the fashion of how the electrons are distributed among Landau levels. The electron distribution may be most simply characterized by an effective electron temperature $T_e(r)$.

Suppose that cold electrons ($T_e \sim 0$) are injected from the wide 2DEG pad region into the narrow 2DEG channel as shown in Fig. 6(a). Since $T_e \sim 0$, both the rate of energy gain $\sigma_{xx}(T_e)E_H^2$ and the rate of energy loss $L(T_e)$ are vanishingly small, and the energy-balance equation $\sigma_{xx}(T_e)E_H^2 = L(T_e)$ can be satisfied in the 2DEG channel. However, this (nearly) dissipationless state can be unstable if the stability condition

$$\left(\frac{\partial \sigma_{xx}}{\partial T_e}\right)E_H^2 < \left(\frac{\partial L}{\partial T_e}\right) \tag{1}$$

is violated at $T_e \sim 0$ by the finite size of E_H.

If so, no matter how small the energy gain rate is, infinitesimal fluctuations in the electron distribution will start developing to elevate T_e during the travel of electrons along the 2DEG channel. The process lasts until a new stable steady state with a higher T_e is reaches, at which stability condition (1) is recovered. This transition is not assisted directly by $E_H(r)$ but occurs in the form of an avalanche-type inter-Landau-level excitation of carriers through Auger-type processes as schematically shown by the arrows with solid lines in Fig. 6(a) [16]. So the transition may be slow in time domain, and electrons may have to travel a macroscopic distance in space before the new stable state is reached to exhibit well-defined breakdown characteristics, as shown in Fig. 6(b)].

In summary, we discovered a remarkable, current-polarity dependent, nonlocal nature of the QHE breakdown. We suggested bootstrap-type electron heating as the relevant mechanism of te QHE breakdown.

This work is supported by the Grants-in-Aid for Scientific Research on Priority Area "Quantum Coherent Electronics" and by the Grants-in-Aid for scientific Research (A), both from the Ministry of Education Science and Culture.

[1] K. von Klitzing, G. Dorda, and M. Pepper, Phys. Rev. Lett. **45**, 449 (1980).
[2] S. Kawaji and J. Wakabayashi, in *Physics in High Magnetic Fields*, edited by S. Chikazumi and N. Miura (Springer, Berlin, 1981), p. 284.
[3] G. Ebert *et al.*, J. Phys. C **16**, 5441 (1983).
[4] M. E. Cage *et al.*, Phys. Rev. Lett. **51**, 1374 (1983).
[5] S. Komiyama *et al.*, Solid State Commun. **54**, 479 (1985).
[6] T. Takamasu *et al.*, Surf. Sci. **170**, 202 (1986).
[7] J. R. Kirtley *et al.*, Phys. Rev. B **34**, 1384 (1986); **34**, 5414 (1986).
[8] L. Bliek *et al.*, Surf. Sci. **196**, 156 (1988).
[9] M. E. Cage *et al.*, Semicond. Sci. Technol. **5**, 351 (1990).
[10] F. J. Ahlers *et al.*, Sci. Technol. **8**, 2062 (1993).
[11] N. Q. Balaban *et al.*, Phys. Rev. Lett. **71**, 1443 (1993).
[12] A. Boisen *et al.*, Phys. Rev. B **50**, 1957 (1994).
[13] S. Kawaji *et al.*, J. Phys. Soc. Jpn. **63**, 2303 (1994).
[14] T. Okuno *et al.*, J. Phys. Soc. Jpn. **64**, 1881 (1995).
[15] N. Q. Balaban, U. Meirav, and H. Shtrikman, Phys. Rev. B **52**, R5503 (1995).
[16] Y. Kawaguchi *et al.*, Jpn. J. Appl. Phys. **34**, 4309 (1995).
[17] Y. Kawaguchi *et al.*, (to be published).
[18] In Fig. 2, the sizes of the longitudinal voltages appearing in the breakdown regime systematically change upon the reversal of B or the interchange of the voltage probes. This can be explained by noting that the Hall resistance is appreciably larger in the breakdown regime than in the QHE regime at $\nu = 2$ [Fig. 3(a)] and that the distribution of the longitudinal electric field is accordingly distorted in the neighborhood of the junction. Note that this systematic difference is not appreciable in the data of Fig. 4.
[19] The critical current ($I_c \approx 10\ \mu$A) is not accurately proportional to the device width ($W = 20\mu$m), when compared to $I_c \approx 3\ \mu$A ($W = 3\mu$m) in Figs. 2 and 5. In fact, I_c in wafer 1 shows a slight sublinear dependence on W [16].
[20] D. C. Tsui, G. J. Dolan, and A. C. Gossard, Bull. Am. Phys. Soc. **28**, 365 (1983).
[21] O. Heinonen, P. L. Taylor, and S. M. Girvin, Phys. Rev. B **30**, 3016 (1984).
[22] L. Eaves and F. W. Sheard, Semicond. Sci. Technol. **1**, 346 (1986).
[23] A. VI. Gurevich and R. G. Mints, Pis'ma Zh. Eksp. Teor. Fiz. **39**, 318 (1984) [Sov. Phys. JETP Lett. **39**, 381 (1984)].